Slack M.D., Prasad R.O., Bakker A., Boysan F. (2000) Advances in Cyclone Modelling Using Unstructured Grids, TransIChemE, Vol. 78, Part A, November 2000, page 1098-1104.

IChemE

0263–8762/00/$10.00+0.00

Trans IChemE, Vol 78, Part A, November 2000

ADVANCES IN CYCLONE MODELLING USING UNSTRUCTURED GRIDS

M. D. SLACK, R. O. PRASAD, A. BAKKER and F. BOYSAN

Fluent Europe Ltd, Sheffield, UK

This paper reviews the application of Computational Fluid Dynamics (CFD) for cyclone modelling on three-dimensional unstructured meshes using both the Reynolds Stress Turbulence model and Large Eddy Simulation. Results of the subsequent numerical simulations show consistent agreement compared with Laser Doppler Anemometry measurements at a series of axial stations throughout the length of a Stairmand high efficiency cyclone.

Keywords: cyclone; CFD; RSM; LES; unstructured; Fluent.

INTRODUCTION

The cyclone separator is perhaps the most widely used separation device to be found in industry. It owes its popularity to the low manufacturing and maintenance costs brought about by its simple design. There are no moving parts in the device itself, which can be constructed from a wide range of materials including refractories for high temperature operation. Combined with moderate pressure drop and a range of throughputs and efficiencies, these advantages have made the cyclone the most attractive solution to separation in both gas-solid and liquid-solid systems.

Cyclones can be distinguished from other separation devices by noting that the centrifugal forces caused by the swirling motion of the flow being the means of separation. In the familiar reverse flow cyclone of cylinder-on-cone design, the fluid spirals down from a tangential inlet towards the apex of the conical section, reversing direction at the bottom, before proceeding upwards in an inner core to exit via the vortex finder.

A considerable amount of experimental data exists on cyclone performance[1,2], obtained for the most part in the 1930s and 1940s, using impact tubes, before the availability of Laser Doppler Anemometry or electronic hot-wire probes, which form the basis of many necessarily semi-empirical correlations on which current design practice is based. The design method usually depends on a number of expressions to obtain an overall pressure drop and a characteristic grade-efficiency curve, as a function of geometrical factors and operating conditions.

In recent years, the advent of powerful digital computers has provided the means whereby mathematical modelling of the fundamental physical processes can be applied to realistic cyclone geometries. However, when CFD is used for design and analysis in typical industrial settings, it is always subjected to some constraints. Amongst practical constraints are the allocable memory and the total amount of CPU time that may be spent on the simulation. These constraints largely determine the total cell count and the modelling approach, the latter being reflected in the choices of the turbulence model and other physical models. For these reasons, previous studies of numerical prediction of cyclone flow fields have mostly been restricted to axi-symmetric geometries[3,4,5], with a few three dimensional simulations being reported only in recent years[6,7,8]. Almost all of these studies use the Reynolds Averaged Navier-Stokes equations (RANS) in time-averaged form, using the Reynolds Stress Modelling (RSM) of turbulence. It has been reported in the literature that the popular $k-\varepsilon$ variety of turbulence models are not suitable for the simulation of highly swirling turbulent flows, such as the one found in cyclone separators[3,5,7]. Mathematical models can, in principle, not only enhance our understanding of the complicated fluid mechanics of the cyclone separator and aid its design, but also can be extrapolated to situations which lie outside present day experience.

This paper presents the results of simulations of flow fields in a Stairmand design cyclone, in three dimensions, using both the Reynolds Stress Model of turbulence and the more recently available Large Eddy Simulation technique. The results are compared with experimentally obtained distributions of velocity components.

SIMULATION STRATEGY

The fidelity of CFD predictions for turbulent flows is highly dependent upon the quality of the turbulence modelling. This is especially true when it comes to the flow in cyclone separators, because the salient features include high swirl, three-dimensional boundary layers with strong streamline curvature. These features require turbulence models that can properly account for anisotropy and non-equilibrium effects.

Surveying recent literature shows that there are numerous engineering turbulence models, ranging from simple algebraic models to second order Reynolds Stress closures (RSM), Large Eddy Simulation (LES) and Direct Numerical Simulation (DNS).

Turbulent flows contain a wide range of length and time scales. In a direct numerical simulation (DNS) of turbulent flows, the Navier-Stokes equations are solved on a fine enough mesh to resolve even the smallest scales of motion. If the numerical scheme is designed to give minimum numerical dissipation and dispersion errors, DNS gives an accurate three-dimensional, time dependent, solution of the

governing equations. DNS has been successfully used in the past few years to study transitional and turbulent flow physics in simple flows. The required number of grid points in each direction for resolving all the scales of motion in turbulence is proportional to the ratio of the size of the large, energy containing and the Kolmogorov scale eddies. This ratio is shown to be proportional[9] to $Re_t^{3/4}$, where Re_t is the turbulent Reynolds number of the flow defined by $Re_t = u' l_t/\nu$, u' is the turbulence intensity and l_t is the integral turbulence length scale. Therefore, the number of grid points required for three-dimensional DNS is proportional to $Re_t^{9/4}$. The overall cost of the computational effort is proportional to Re_t^3. Therefore, an eight-fold increment in computational resources is required to increase the permissible turbulence Reynolds number for DNS by a factor of two[9].

Considering the computational resources needed for conducting DNS, some form of modelled equations must be used in industrial simulations. In most instances, the Reynolds averaged Navier-Stokes equations (RANS) approach is used. In this approach, the governing equations are averaged over a time period much larger than the time scales of the turbulent fluctuations, and the resulting equations are numerically integrated. The averaging procedure results in additional terms, called Reynolds stresses, because of the nonlinearity of the convective terms. The Reynolds stresses must be modelled approximately. In general, industrial simulations of turbulent flows are conducted using the two-equation or Reynolds stress turbulence models (RSM). The constants in these models are obtained using the experimental data from simple shear flows. While these models provide solutions of engineering accuracy for a range of flows, they lack generality due to the fact that the models based on the RANS approach must represent a wide range of scales of turbulence and the large scales are strongly dependent on boundary conditions. The equations of RSM have been reported elsewhere and will not be repeated here[10].

Recently, the large eddy simulation (LES) approach has been used for a wide range of flows[9]. In this approach, the governing equations are obtained by spatially filtering the Navier-Stokes equations. The large turbulent scales are computed explicitly, while the small scales are modelled using subgrid scale (SGS) models. The SGS models describe interactions between the resolved and unresolved scales. The LES approach avoids the oft-quoted weakness of the RANS approach, that the models based on this approach must represent a wide range of scales of turbulence and the large scales are strongly dependent on boundary conditions. Similar to direct numerical simulations (DNS), the LES approach gives a three-dimensional, time dependent solution. This method needs computational resources that are intermediate between those required by the DNS and RANS approaches. The LES can be used at much higher Reynolds numbers than DNS, as the computational effort is independent of the Reynolds number if the small scales obey the inertial range spectrum and the near wall effects are not important.

MATHEMATICAL FORMULATION

Governing Equations

The governing equations for LES are obtained by spatially filtering over small scales. The effect of small scales on large scales is represented by SGS models. A generic filtered variable, $\tilde{f}$, is defined as:

$$\bar{\rho}(\mathbf{x})\tilde{f}(\mathbf{x}) = \int_D \rho(\mathbf{x}')f(\mathbf{x}')G(\mathbf{x}-\mathbf{x}')\mathrm{d}\mathbf{x}' \tag{1}$$

where $\mathbf{x}$ and $\mathbf{x}'$ are spatial coordinates in the domain D and G is the filter function. In spectral methods for solving the governing equations, a sharp Fourier cut-off filter is used. In finite volume methods, a top-hat filter of the following form is often used.

$$\begin{aligned} G(\mathbf{x}-\mathbf{x}') &= \frac{1}{\Delta_x\Delta_y\Delta_z} \text{ if} |\mathbf{x}-\mathbf{x}'| \le \Delta/2 \\ &= 0 \qquad \text{otherwise} \end{aligned} \tag{2}$$

where Δ_x, Δ_y and Δ_z are filter widths in the three coordinate directions. In the current study, a top-hat filter of filter width to grid size ratio of two is used. With this filter, differentiation and filtering operations commute only on uniform grids. The importance of commutation errors on nonuniform grids is a topic of the current research, and in the present work it is assumed that the commutation error is a part of the error in the subgrid models.

Applying the filtering operation to the continuity, momentum, species and energy equations, gives:

$$\frac{\partial\bar{\rho}}{\partial t} + \frac{\partial\bar{\rho}\tilde{u}_j}{\partial x_j} = 0 \tag{3}$$

$$\frac{\partial\bar{\rho}\tilde{u}_i}{\partial t} + \frac{\partial\bar{\rho}\tilde{u}_1\tilde{u}_j}{\partial x_j} = -\frac{\partial\bar{p}}{\partial x_i} + \frac{\partial\bar{\tau}_{ij}}{\partial x_j} + \frac{\partial\sigma_{ij}}{\partial x_j} \tag{4}$$

where $\bar{\tau}_{ij}$ is the filtered stress sensor given by:

$$\bar{\tau}_{ij} = -\frac{2}{3}\mu(\tilde{T})\delta_{ij}\frac{\partial\tilde{u}_k}{\partial x_k} + \mu(\tilde{T})\left(\frac{\partial\tilde{u}_1}{\partial x_j} + \frac{\partial\tilde{u}_j}{\partial x_i}\right) \tag{5}$$

In the filtered equations, the terms represented by σ_{ij}, called SGS stresses/fluxes, are described below:

$$\sigma_{ij} = -(\overline{\rho u_i u_j} - \bar{\rho}\tilde{u}_i\tilde{u}_j) \tag{6}$$

The SGS stresses/fluxes need to be modelled.

Subgrid Turbulence Model

In the filtered equations, the terms represented by σ_{ij} are called subgrid scale (SGS) stresses, and need to be modelled. Yakhot *et al.*[11] have obtained a RNG subgrid scale stress model by performing recursive elimination of infinitesimal bands of small scales. In the RNG SGS model, subgrid fluxes in the momentum equation are represented by:

$$\sigma_{ij} - \frac{1}{3}\sigma_{kk}\delta_{ij} = 2\mu_{sgs}\tilde{S}_{ij} \tag{7}$$

This model differs from the Smagorinsky[12] model in the way subgrid viscosity is calculated. In the RNG subgrid model, the total viscosity, $\mu_{tot} = \mu + \mu_{sgs}$, is given by

$$\mu_{tot} = \mu\left[1 + H\left(\frac{\mu_{sgs}^2\mu_{tot}}{\mu^3} - C\right)\right]^{1/3} \tag{8}$$

where $\mu_{sgs} = \bar{\rho}(C_m\Delta)^2(2S_{ij}S_{ij})^{1/2}$, $H(x)$ is the Heaviside ramp function. The coefficients, $C_S = 0.157$ and $C = 100$ are obtained from the theory. When the filtering operation results in very high subgrid viscosity compared to the

molecular viscosity, $\mu_{tot} = \mu_{sgs}$, and the RNG theory based subgrid scale model returns to the Smagorinsky model form. If $\mu_{sgs} \approx 0$, the argument of the Heaviside function is negative and the total viscosity is equal to molecular viscosity. This model correctly yields zero SGS viscosity in low Reynold number flows without any *ad hoc* modifications.

Numerical Method

The numerical simulations are conducted using FLUENT V5. A detailed discussion of the numerical method and several validation studies of this code are given by Mathur and Murthy[13]. In this code, the domain is discretized into arbitrary unstructured polyhedra. The discretized form of the governing equations for each cell is obtained such that the conservation principles are obeyed on each polyhedron. The resulting discretized equations for the variable φ are given by:

$$a_p \varphi_p = \sum_{nb} a_{nb} \varphi_{nb} + S_p \tag{9}$$

The summation in equation (20) extends over all the neighbour cells of cell p, i.e. all the cells, which share a face with the cell p. The number of cell neighbours in equation (9) is arbitrary for unstructured meshes. Therefore, normal line-iterative solvers cannot be used. In FLUENT, the linear equations are solved using an algebraic multigrid procedure developed by Hutchinson and Raithby[14], more details of the algebraic multigrids used on unstructured meshes may be found in Mathur and Murthy[13]. FLUENT V5 uses colocated meshes considering their well-known advantages over staggered meshes for complex geometries. Checkerboarding of pressure and velocity fields on the colocated meshes is avoided by a momentum interpolation procedure[13]. The SIMPLE algorithm is used for coupling the continuity and momentum equations[15]. All the results presented in this section are obtained using a third order accurate QUICK scheme for spatial discretization[16]. The time-advancement is made with a second-order accurate implicit scheme. This scheme uses information from two previous time steps to calculate the time derivative.

RESULTS

The experimental cyclone configuration is depicted in Figure 1, a typical high-efficiency cyclone design of Stairmand[1]; in this case having a diameter D of 0.205 m. The volume of the cyclone was 0.0203 m^3. Incompressible flow with a density of air of 1.225 $kg\,m^{-3}$ and a viscosity of 1.7894E-05 $kg\,m^{-1}\,s^{-1}$ was assumed. The volumetric flow rate through the cyclone was 0.08 $m^3\,s^{-1}$, resulting in an average residence time of 0.25 s.

Radial profiles of axial and tangential velocities have been measured using a backscatter LDA system. The experimental data were reported previously[17,18]. The cyclone inlet velocity used in the simulation corresponds to the airflow rate of 0.08 $m^3\,s^{-1}$, extrapolated from LDA measurements taken across the inlet of the cyclone. A relatively coarse unstructured grid has been used with approximately 40,000 cells for the Reynolds stress simulations shown in Figure 2.

The flow field generated from the calculations using the RSM model is shown in Figure 3 (for clarity the azimuthal

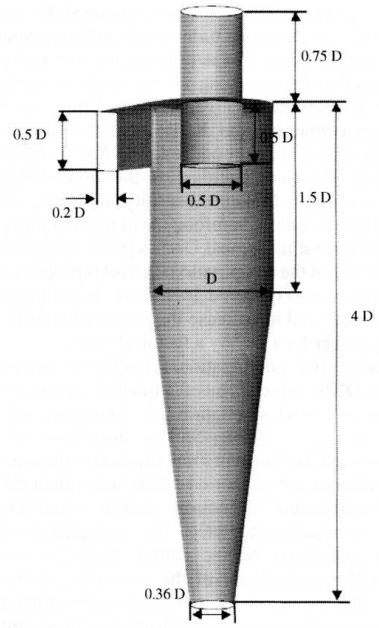

Figure 1. Outline of Stairmand cyclone showing non-dimensionalized dimensions.

components of velocity have been suppressed). It can be seen that the flow forms descending and ascending streams, which flow parallel to one another before leaving the cyclone through the vortex tube. This behaviour is expected and is due to the fact that swirling flows have a tendency to resist radial motion, which gives rise to several other features. After entering the cyclone, the main body of the flow forms a stream, which flows along the outer wall towards the bottom, and accelerates due to area reduction. Upon reaching the bottom of the cyclone, this stream changes direction and moves towards the vortex tube.

Axial stations 0.32, 0.35, 0.38, 0.41, 0.59, 0.62, 0.66, 0.77, 0.8 are compared with predicted tangential and axial

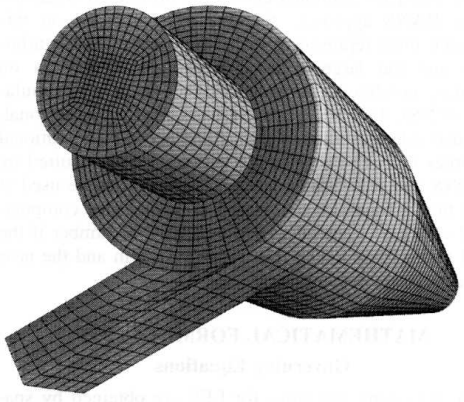

Figure 2. Unstructured hexahedral mesh.

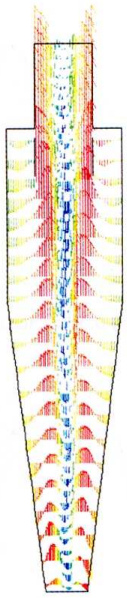

Figure 3. Axial velocity vectors in the CFD simulation.

velocity profiles at equivalent locations in the CFD simulation, see Figures 5, 6, and 7. The flow field simulation has adequately predicted the axial and tangential components of the flow in the one plane. It is imperative that the swirl velocity (tangential component) is predicted correctly in order to accurately reproduce the rest of the flow field. The swirling flow is shown by means of pathlines in Figure 4. The results of the numerical simulation for both axial and tangential velocity show consistent agreement with the LDA measurements down the length of the cyclone.

For the LES simulation, a finer grid of approximately

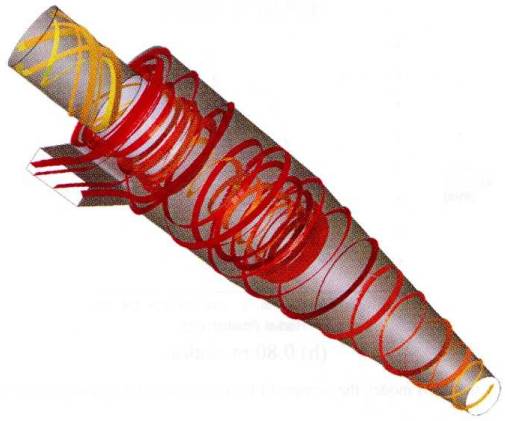

Figure 4. Pathlines showing the spiral flow in a cyclone.

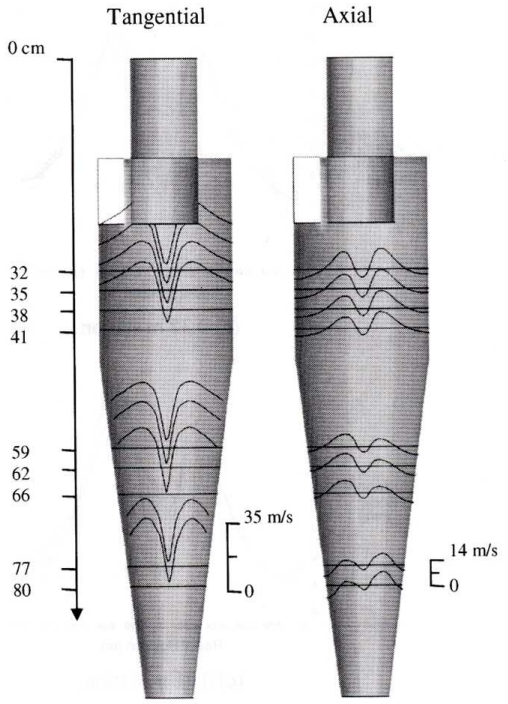

Figure 5. Predicted tangential and axial velocity distributions at each of the axial stations in the high-efficiency cyclone of Stairmand using the RSM model.

640,000 cells was constructed. The simulation was started with a steady state RSM solution as an initial condition. A period of 0.5 s, corresponding to two residence times, was simulated using a time step of 5E-5 s. Figure 8 shows local velocity magnitude, velocity vectors and axial vorticity in the cyclone at intervals of 8.4E-3 s, near the end of the simulation. It is clear that the central vortex in the cyclone is not steady, but exhibits semi-periodic oscillations. These oscillations are averaged out in the steady state RSM calculations. Thus, the LES calculations provide additional detail about the flow in the cyclone that cannot be obtained otherwise. Such oscillations may potentially affect the separation efficiency of the cyclone and wall erosion, and have also been observed experimentally[19,20].

Figures 5 and 6 also include the LES results. The RSM predictions are slightly better at the first locations ($y = -0.32$, -0.38 and -0.41 m) while the averaged LES gives slightly better predictions at the remaining five locations. Overall, the averaged LES results compare slightly better with the experimental data than do the RSM results, but it required a finer mesh and longer computational time. To explain the discrepancy in the LES results at the first three locations, considering Figure 8, the results show that the unstable motion of the central core fluctuates much faster in the lower tapered section of the cyclone. Therefore, the time averaged LES results incorporate more periods of motion in the lower section. While those in the upper section average about 2.5 periods of motion, biasing the result. This is a useful observation to be borne in mind

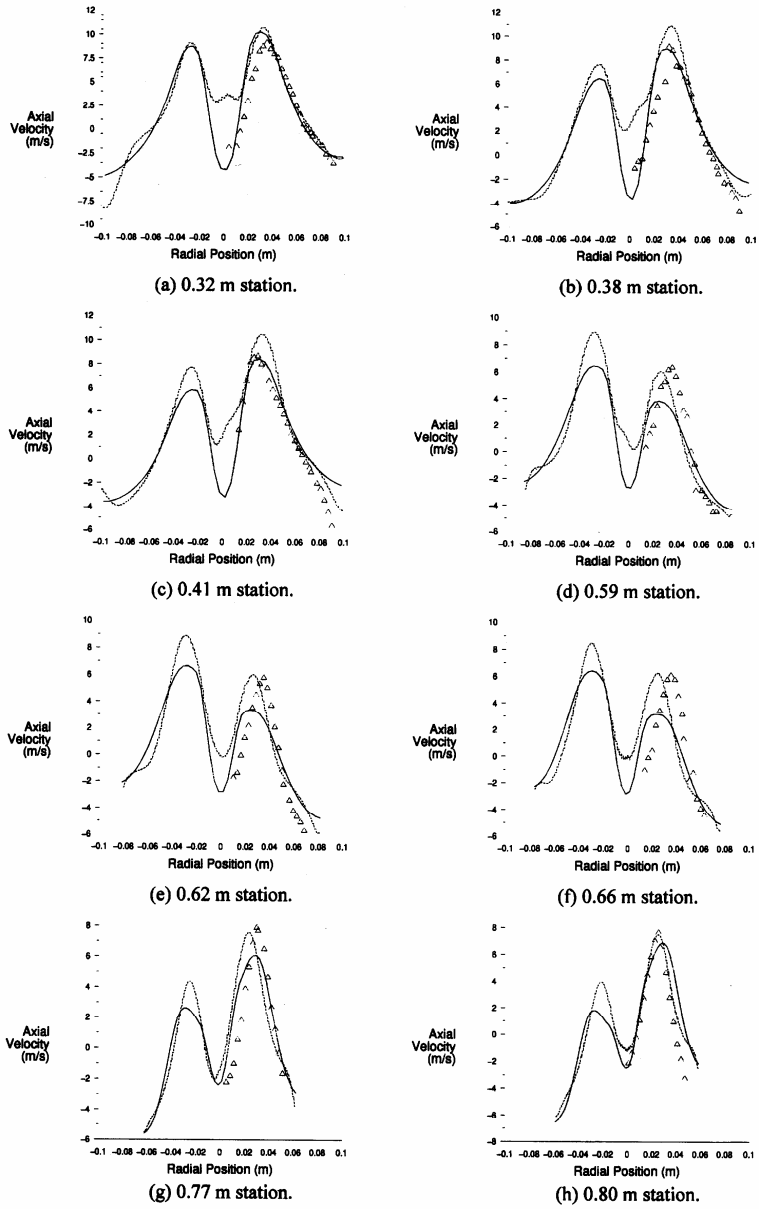

Figure 6. Comparison between the axial velocity at various stations as predicted by the RSM model, the averaged LES results, and the experimental data (△ Experimental data; — RSM model; - - - Time averaged LES results).

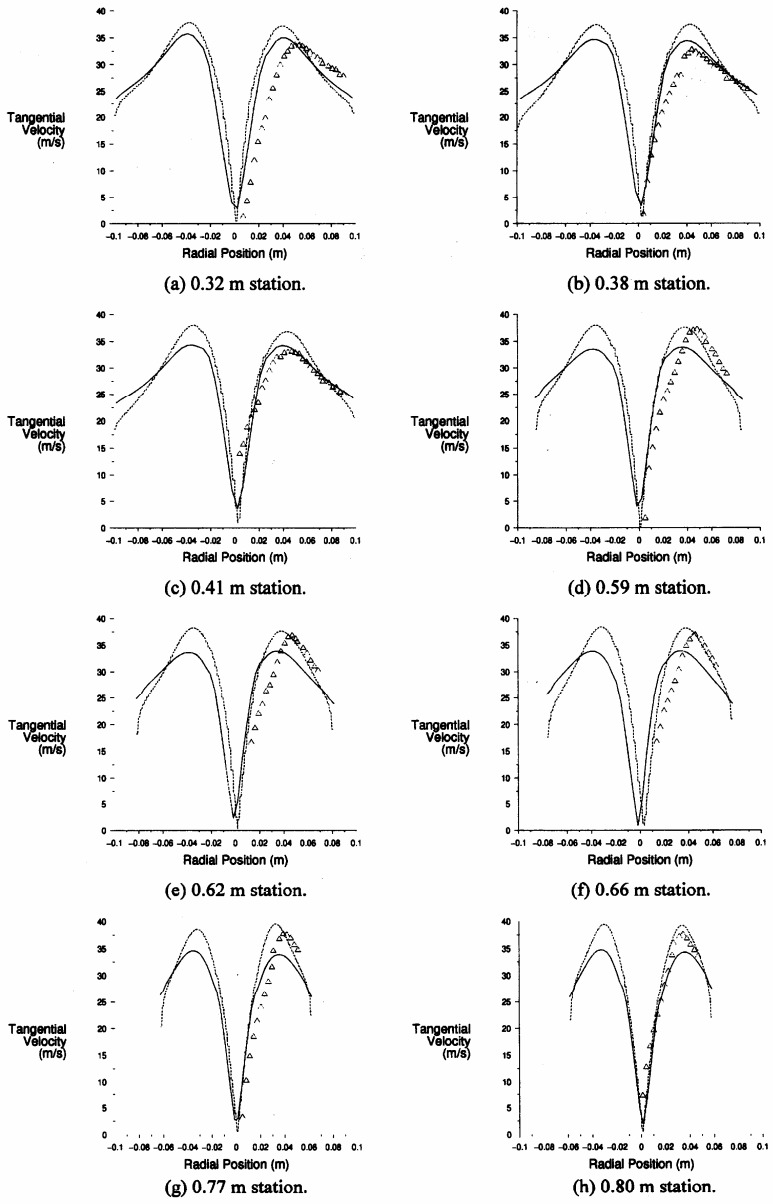

Figure 7. Comparison between the tangential velocity at various stations as predicted by the RSM model, the time averaged LES results, and the experimental data (Δ Experimental data; — RSM model; - - - Time averaged LES results).

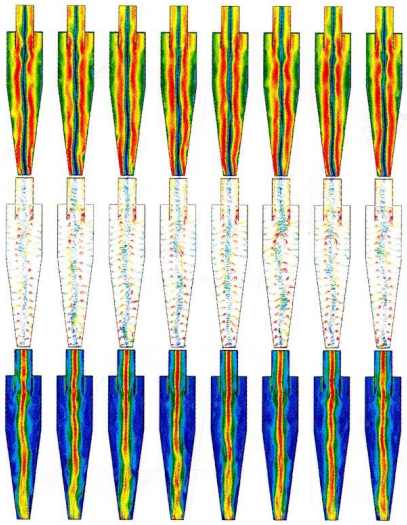

Figure 8. Flow pattern results from the time dependent LES simulations. The top row shows local velocity magnitude (red is 45 m s^{-1} or higher, blue is 5 m s^{-1} or lower), the centre row shows local velocity vectors, and the bottom row shows axial vorticity (red is 5550 s^{-1} or higher and blue is 1000 s^{-1} or lower). Images are shown at intervals of 8.4 ms. The first column of images is at $t = 0.26895$ s and the last column is at $t = 0.32775$ s.

when comparing any time averaged LES data. A model and discussion of processing vortex harmonics is presented in the paper by Sozou and Swithenbank[21].

Large **E**ddy **S**imulation turbulence modelling lends itself well to the cyclone, the short residence times of the fluid mean that there is little time for the turbulent energy to diffuse down the energy cascade to the smaller eddies. The behaviour is therefore dominated by the larger eddies placing less importance on the choice of subgrid scale model used.

CONCLUSIONS

The flow field in a conventional high efficiency Stairmand cyclone was successfully modelled using an unstructured mesh and using both RSM and LES turbulence models. The results show an excellent agreement between predicted and experimental measurements at all of the axial stations considered. Steady state simulations using a Reynolds stress turbulence model on a relatively coarse unstructured mesh provides a computationally inexpensive method for examining in detail the time-averaged flow field in cyclonic flows of this type. The computationally more expensive large eddy simulation model on a finer mesh reveals time dependent vortex oscillations, which potentially impact the separation efficiency and wall erosion. This will be the subject of further study. CFD lends itself to the development of new and innovative designs that may be outside of the usual scope.

REFERENCES

1. Stairmand, C. J., 1951, The design and performance of cyclone separators, *Trans IChemE*, 29: 356–383.
2. Kelsall, D. F., 1952, A study of the motion of solid particles in a hydraulic cyclone, *Trans IChemE*, 30: 87–108.
3. Boysan, F., Ayers, W. H. and Swithenbank, J., 1982, A fundamental mathematical modelling approach to cyclone design, *Trans IChemE*, 60: 222–230.
4. Boysan, F., Swithenbank, J. and Ayers, W. H., 1996, Mathematical modeling of gas-particle flows in cyclone separators, *Encyclopedia of Fluid Mechanics, Volume 4—Solids and Gas Flows*, Chapter 42, pp. 1307–1329 (Gulf Publishing, ISBN 0 87201-516-5).
5. Davidson, M. R., 1988, Numerical calculations of flow in a hydrocyclone operating without an air core, *Appl Math Modelling*, 12: 119–128.
6. Cristea, E. D., Malfa, E. and Coghe, A., 1994, *3D Simulation and Experiments of Cement Rotary Kiln Preheater Top Cyclone, Fluent Users Group Meeting UK*.
7. Slack, M. D. and Wraith, A. E., 1997, Modelling the velocity distribution in a hydrocyclone, *4th Int Colloq on Process Simulation*, 65–83.
8. Hoekstra, A. J., Derksen, J. J. and Van den Akker, H. E. A., 1999, An experimental and numerical study of turbulent swirling flow in gas cyclones, *Chem Eng Sci*, 54: 2055–2065.
9. Reynolds, W. C., 1990, The potential and limitation of direct and large eddy simulations, in *Wither Turbulence? Turbulence at the Cross-roads*, (Ed. J. L. Lumley), 313–342.
10. Leschziner, M. A., 1990, Modelling engineering flows with Reynolds-stress turbulence closure, *J Wind Eng and Indust Aero*, 35(1–3): 21–47.
11. Yakhot, A., Orszag, S. A., Yakhot, V. and Israeli, M., 1986, Renormalization Group Formulation of Large-Eddy Simulation, *J Scientific Computing*, 1: 1–51.
12. Smagorinsky, J., 1963, General circulation experiments with the primitive equations, I. The basic experiment, *Month Wea Rev*, 91: 99–164.
13. Mathur, S. R. and Murthy, J. Y., 1997, A pressure-based method for unstructured meshes, numerical heat transfer, *Part B*, 31: 195–215.
14. Hutchinson, B. R. and Raithby, G. D., 1986, A multigrid method based on the additive correction strategy, *Numerical Heat Transfer*, 9: 511–537.
15. Patankar, S. V., 1980, *Numerical Heat Transfer and Fluid Flow* (Hemisphere Publishing Corporation).
16. Leonard, B. P. and Mokhtari, S., 1990, Ultra-sharp nonoscillatory convection schemes for high-speed steady multidimensional flow, *NASA TM 1-2568 (ICOMP-90-12)* (NASA Lewis Research Center).
17. Boysan, F., Ewan, B. C. R., Swithenbank, J. and Ayers, W. H., 1983, Experimental and theoretical studies of cyclone separator aerodynamics, *IChemE Symp Series*, No 69: 305–320.
18. Ayers, W. H., Boysan, F., Swithenbank, J. and Ewan, C. R., January/February 1985, Theoretical modeling of cyclone performance, *Filtration & Separation*: 39–43.
19. O'Doherty, T., Griffiths, A. J., Syred, N. and Bowen, P. J., 1999, Experimental analysis of rotating instabilities in swirling and cyclonic flows, *Dev Chem Eng Mineral Process*, 7(3/4): 245–267.
20. Griffiths, A. J., Yazdabadi, P. A. and Syred, N., 1998, Alternate eddy shedding set up by the nonaxisymmetric recirculation zone at the exhaust of a cyclone dust separator, *J Fluids Eng*, 120: 193–199.
21. Sozou, C. and Swithenbank, J., 1969, Adiabatic waves in a rotating fluid, *J Fluid Mech*, 38(4): 657–671.

ACKNOWLEDGEMENTS

The authors would like to thank Dr Elizabeth Marshall for her help compiling this paper.

ADDRESS

Correspondence concerning this paper should be addressed to Dr M. D. Slack, Fluent Europe Ltd, Sheffield Airport Business Park, Europa Link, Sheffield S9 1XU, UK.

The manuscript was received 6 April 2000 and accepted for publication after revision 5 July 2000.